SOURCE FUNCTION IN A NON-EQUILIBRIUM ATMOSPHERE
III. THE INFLUENCE OF A CHROMOSPHERE

JOHN T. JEFFERIES AND RICHARD N. THOMAS
Boulder Laboratories, National Bureau of Standards, High Altitude Observatory, and Sacramento Peak Observatory
Received September 29, 1958

ABSTRACT

We apply the methods developed in the preceding two papers to investigate the depth dependence of the source function for resonance lines in an atmosphere having a chromospheric distribution of T_e superposed upon a photospheric one. The derived behavior of $S_L(\tau)$ for the neutral and ionized metals differs and mimics the observed behavior of such lines. The hydrogen Balmer lines should behave like the neutral metals, and the predicted behavior agrees with our earlier empirical results.

I. INTRODUCTION

Paper I of this series (Thomas 1957) presented three main results: (i) the line source function, S_L, for resonance lines is effectively frequency-independent over a central core some three Doppler widths in extent; (ii) an algebraic expression derived for S_L (cf. eq. [1]) shows that for the analysis of resonance lines a very good approximation to the behavior of S_L results from considering the two discrete levels plus the continuum; (iii) resonance lines can, in general, be divided into two classes according to the predominance of a collision term, $\epsilon B_\nu(T_e)$ or of a photoelectric ionization term, $\mathfrak{L}$, as a "source" term added to the scattering term in this expression for S_L.

In Paper II (Jefferies and Thomas 1958) we suggested a method for determining the depth dependence of S_L and applied the method, for the case of collisionally excited lines, to an atmosphere with a photospheric-type distribution of T_e. This work showed that, for the adopted temperature distribution, $S_L(T_e)$ is less than $B_\nu(T_e)$ at the same atmospheric position, with the difference increasing toward the top of the atmosphere.

In the present paper we apply the methods of Paper II to investigate the above S_L for both classes of lines, with a distribution of T_e that mimics both photosphere and chromosphere. We show (i) that the essential features of a self-reversed emission core, such as those exhibited by the H and K lines, are predicted from a collision-type S_L coupled with a chromospheric rise in T_e; (ii) that, by contrast, the photoelectric-type S_L should show no such emission core so long as the free-bound opacity of the chromosphere is low but should exhibit an S_L decreasing monotonically outward, although exceeding $B_\nu(T_e)$ in the lower atmosphere; (iii) that, contrary to our suggestion in Paper II, the behavior of the Balmer lines S_L should follow that of a photoelectric-type S_L in the Doppler core and that an $S_L(\tau_C)$ predicted upon such a basis mimics the behavior of the empirical results.

II. COMPUTATION OF $S_L(\tau)$

a) Algebra

For an atom with two discrete levels and a continuum we have, from Paper I,

$$S_L = \frac{\int \bar{I}_\nu \varphi_\nu d\nu + \epsilon B_{\nu_0}(T_e) + \mathfrak{L}}{1 + \epsilon + \eta}, \tag{1}$$

with

$$\epsilon = 0.7 \times 10^{11} Q_{12} n_e T_e^{1/2} (1 + X_{12}) (1 - e^{-X_{12}}) \nu_{12}^{-2} f_{12}^{-1}, \tag{2}$$

$$\eta = 2\,\frac{R^2}{\varpi_1 f_{12}\nu_{12}^2}\,\frac{W_{\kappa 1}}{n_1^3 Z^2}\,\frac{e^{-Y_1}}{Y_1}\,(e^{Y_1-Y_2}-1)\,, \tag{3}$$

and

$$\mathfrak{L} = \eta\,\frac{2h\nu^3}{c^2}\,(e^{Y_1-Y_2}-1)^{-1} \equiv \eta B^*\,, \tag{4}$$

where n_k is the principal quantum number of level k; X_k and Y_k represent the ionization energy from the level k in units of kT_e and kT_r, respectively; T_r represents a radiation temperature in the free-bound continuum with corresponding dilution factor W_κ; and subscripts 2 and 1 denote upper and lower level of the line considered. The expression for η differs algebraically from that given in Paper I, because we have eliminated the non-equilibrium factors b_k by solving explicitly the statistically steady-state case of the pseudo-atom having two discrete levels plus continuum. In the algebraic expressions (3) and (4), certain terms contributing less than some 10 per cent to $\mathfrak{L}$ and η have been dropped.

To solve for the integral term in $S_L(\tau)$, we use the Eddington approximation, as in Paper II,

$$\frac{1}{3}\,\frac{d^2\bar{I}_\nu}{d\tau_\nu^2} = \bar{I}_\nu - \frac{S_L + r_\nu S_C}{1+r_\nu}\,, \tag{5}$$

where S_C is the source function in the continuum, for which we assume the form

$$S_C = B_\nu(T_e) = S_1(1+\beta\tau_0 + A\,e^{-c\tau_0})\,, \tag{6}$$

τ_0 being the optical depth at the line center, $\beta = 1.5r_0$, and r_ν the ratio of the opacity in the continuum to that in the line.

To solve equation (3), we suppose r_ν, $\mathfrak{L}$, ϵ, and η to be independent of depth. Substituting equations (1) and (6) in (5) and, as in Paper II, replacing the frequency integral by a Gaussian quadrature, equation (5) reduces to a set of simultaneous equations, from which S_L follows as below.

Collisional S_L, i.e., $\eta = 0$:

$$S_L = S_1\left\{1+\beta\tau_0 + A\,[\gamma + (1-\gamma)\,q]\,e^{-c\tau_0} + (1-\gamma)\sum_j L_j e^{-k_j\tau_0}\right\}, \tag{7}$$

with the L_j's determined by the boundary condition

$$1 - \frac{\beta}{x_i} + \frac{A\,[1+\varpi_i(q-1)]}{1-c/x_i} + \sum_j \frac{\varpi_i L_j}{1-k_j/x_i} = 0\,. \tag{8}$$

Photoelectric S_L, i.e., $\epsilon = 0$:

$$S_L = S_1(1-u)\left\{1+\beta\tau_0 + \frac{\mathfrak{L}}{S_1} + \left[\frac{\mathfrak{L}}{S_1} - \eta\,(1+\beta\tau_0)\right]\frac{\Sigma a_j v_j}{1-\Sigma a_j V_j} + A\,p\,e^{-c\tau_0} + \sum_j L_j e^{-k_j\tau_0}\right\}, \tag{9}$$

with boundary conditions for the L_j:

$$1 - \frac{\beta}{x_i} + \frac{v_i}{1-\Sigma v_j a_j}\left[\frac{\mathfrak{L}}{S_1} - \eta\left(1-\frac{\beta}{x_i}\right)\right] + A\,\frac{v_i p + w_i}{1-c/x_i} + \sum_j \frac{v_i a_j}{1-k_j/x_i} = 0\,, \tag{10}$$

where the k_j's are determined by

$$\sum_i \frac{y_i a_i}{1 - k^2/x_i^2} = 1 \qquad \begin{cases} y_i = \varpi_i : \text{collisional} , \\ y_i = v_i : \text{photoelectric} , \end{cases} \tag{11}$$

and the symbols are defined by

$$\int \bar{I}_\nu \varphi_\nu d\nu = \sum_1^n \bar{I}_i a_i ; \qquad x_i^2 = 3\phi_i^2 (1 + r_i)^2 ; \qquad \phi_i = \varphi_i \pi^{1/2} \Delta\nu_D ; \qquad r_0 = r_i \phi_i ;$$

$$\gamma = \frac{\epsilon}{1+\epsilon} ; \qquad u = \frac{\eta}{1+\eta} ; \quad \varpi_i = \frac{1-\gamma}{1+r_i} ; \qquad v_i = \frac{1-u}{1+r_i} ; \qquad w_i = \frac{r_i}{1+r_i} ; \tag{12}$$

$$q = \left[\Sigma \frac{a_i (1 - \varpi_i)}{1 - c^2/x_i^2}\right]\left(1 - \Sigma \frac{a_i \varpi_i}{1 - c^2/x_i^2}\right)^{-1} ;$$

$$p = \left(\Sigma \frac{a_i w_i}{1 - c^2/x_i^2}\right)\left(1 - \Sigma \frac{a_i v_i}{1 - c^2/x_i^2}\right)^{-1} .$$

b) Numerical Results

To fix A, S_1, and c, we specify the temperature of the upper solar atmosphere, T_e(max.); the minimum temperature, T_e(min.); and the location of the latter in terms of optical depth in the continuum, τ_{Cm}. We have the relations

$$A \sim R (1 + 1.5 \tau_{Cm}) , \quad R = \frac{B_\nu (T_e \text{ max.})}{B_\nu (T_e \text{ min.})} ,$$

$$\frac{c}{r_0} = \tau_{Cm}^{-1} \left\{\ln [R (\tau_{Cm} + \tfrac{2}{3})] + \ln \frac{c}{r_0}\right\} , \quad S_1 \sim B_\nu (T_e \text{ min.}) . \tag{13}$$

For the sun, T_e(min.) $\sim 4000° \pm 500°$. Using the value 4000°, we obtain values of A and c/r_0 corresponding, respectively, to a range of values for T_e(max.) and τ_{Cm} of current solar interest, as given in the accompanying table.

T_e (max)	A	τ_{Cm}	c/r_0
$1\ 10^4$	25	0.001	1.5×10^4
2.10^4	120	.01	1.28×10^3
5.10^4	430	0 03	4.0×10^2
1.10^5	1000		

Figures 1 and 2 illustrate $S_L(\tau_C)$ and $I_\nu(0)$ for the cases $\epsilon = 10^{-4}$, $r_0 = 10^{-4}$, $\tau_{Cm} = 0.01$, and a range in A. The values chosen correspond to a strong line, such as the H and K lines of Ca^+.

The behavior of S_L for the photoelectric case in which η and B^* are constant is similar to that for the collisional case with constant T_e, for we have

$$S_L = \frac{\int \bar{I}_\nu \varphi_\nu d\nu + \eta B^*}{1 + \eta} . \tag{14}$$

The difference in the two cases comes about because B^* is not, in general, the same as $B_\nu(T_e)$; thus S_L does not couple directly to S_C. The coupling comes about only in the

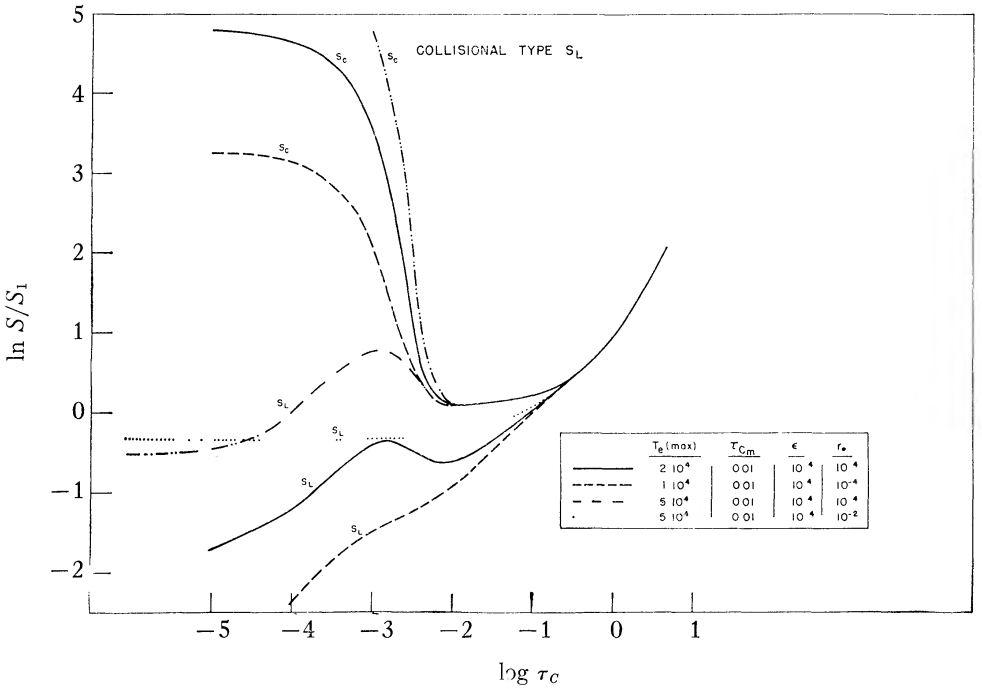

FIG. 1.—$S_L(\tau_C)$ relative to $S_C(\tau_C)$ for a collisional-type source function

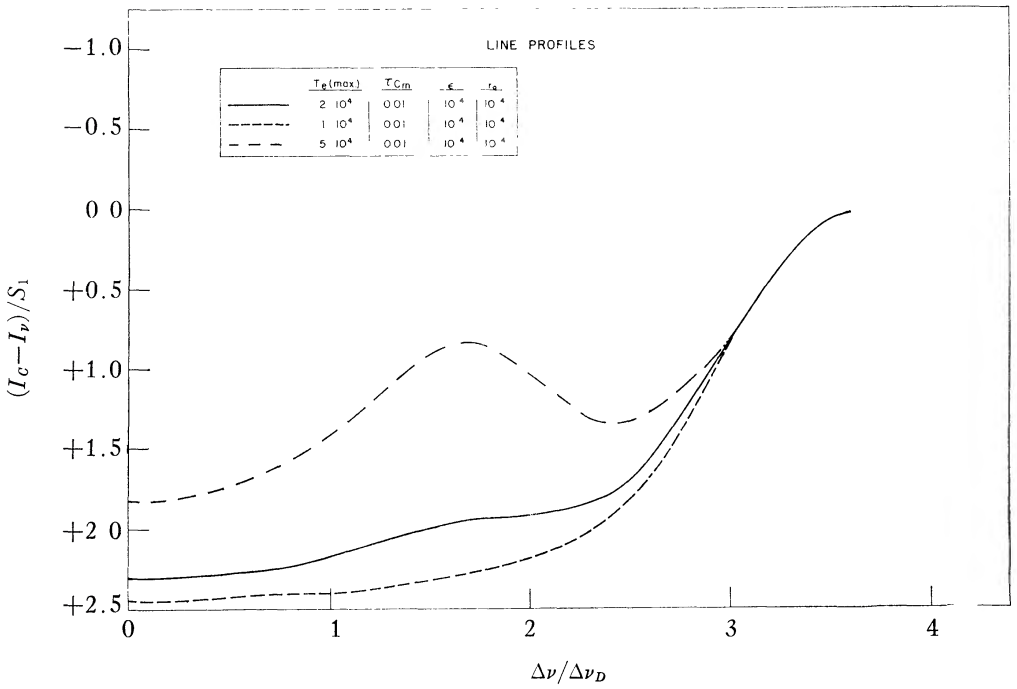

FIG. 2.—Line profiles corresponding to $S_L(\tau_C)$ of Fig. 1

regions deeper than those where our approximation of constant B^* is valid; in the deeper regions B^* approaches $B_\nu(T_e)$.

In the extreme case $r_0 = 0$, we obtain directly from Paper II, or equation (5) with $A = 0$,

$$S_L = B^*\left(1 + \sum_j L_j e^{-k_j \tau_0}\right), \tag{15}$$

and S_L asymptotically approaches B^* from below. Our approximation of constant B^* is valid only in those atmospheric regions having low free-bound opacity. Provided that such regions occur in that part of the atmosphere where T_e is decreasing outward, we see that in the lower part of the atmosphere $S_L > B_\nu(T_e)$. In the upper regions, of course, the inequality reverses.

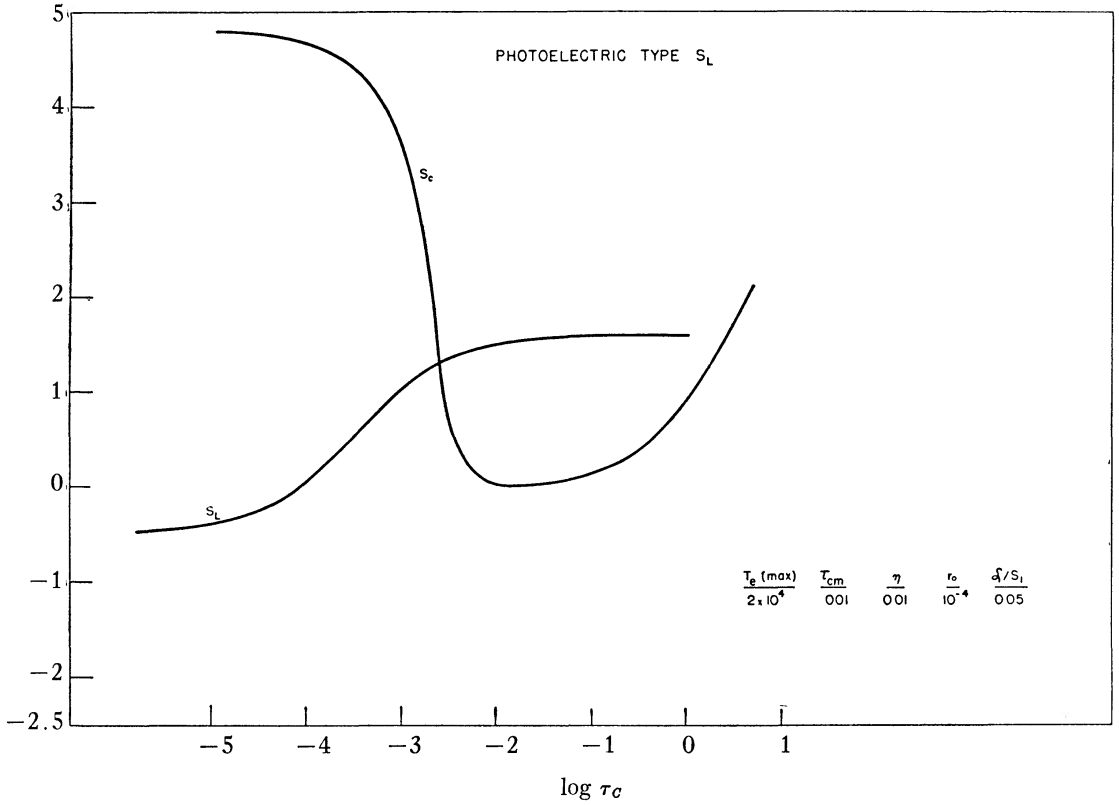

FIG. 3.—$S_L(\tau_C)$ relative to $S_C(\tau_C)$ for a photoelectric-type source function

One may show that the same relative behavior of S_L versus $S_C = B_\nu(T_e)$ holds for the case $r_0 > 0$, by considering the signs of the terms in equation (10). One can show by numerical computation that the result holds for all $A \lesssim 600$ [T_e (max.) $\lesssim 7.10^4$]. Simply for illustration, we present the solution for $\mathfrak{L}/S_1 = 0.05$, $\eta = 0.01$, and $r_0 = 10^{-4}$ in Figure 3.

III. APPLICATION

a) General Results

From the results in Section II we see that the two types of source function—collisional and photoelectric—give rise to two different types of behavior of $S_L(\tau)$, provided that the star has a chromosphere. The collisional S_L introduces the possibility of an emission core, which may be self-reversed; the photoelectric S_L will have no such emission core

so long as the chromosphere has low free-bound opacity. However, if the star has no chromosphere, both types of source functions show the same type of behavior, i.e., no emission core, although, of course, the numerical behavior will differ. In general, as pointed out in Paper I, these two types of behavior should be characteristic of the singly ionized and neutral metals, respectively, with the behavior of other lines yet to be discussed.

If, for example, we consider the Ca^+ H and K lines, on the one hand, and the Na D line, on the other, in the solar Fraunhofer spectrum, we find just this behavior. Thus we conclude that we understand the qualitative behavior of the source function for these

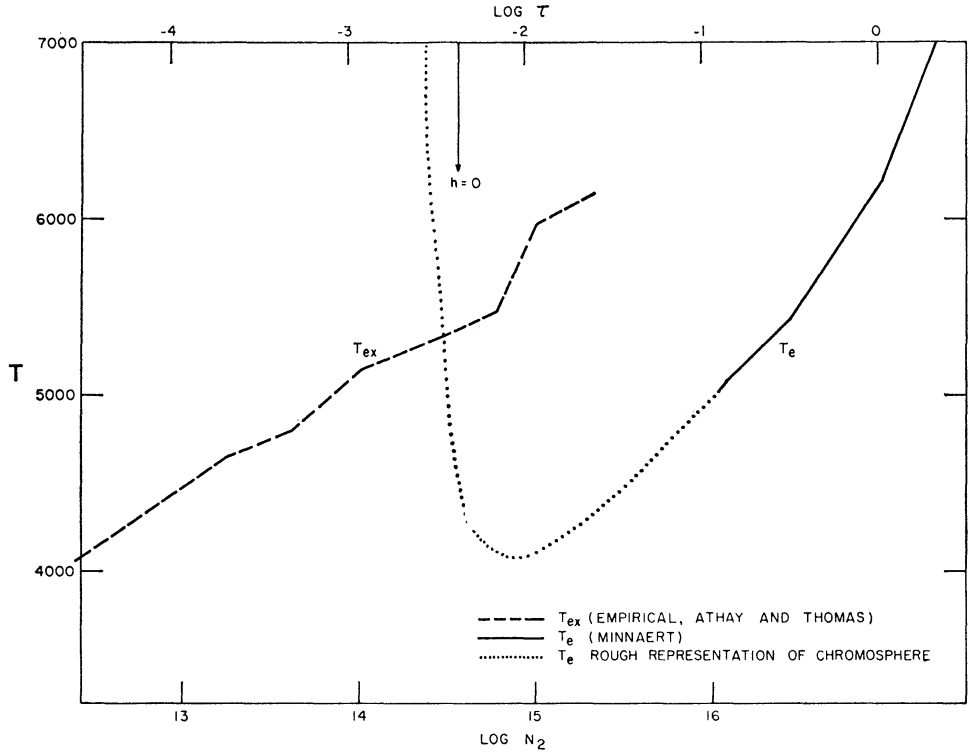

FIG. 4.—Comparison of T_{ex} (empirical) versus log N_2 for Balmer lines (Athay and Thomas 1958) with T_e (Minnaert 1955) for $\tau_{5000} > 0.1$ modified for $\tau < 0.1$ by taking T_e (max.) = 20000° and T_e (min.) = 4000° at $\tau_{5000} = 0.01$.

important classes of lines in the solar spectrum. Furthermore, so long as the emission core of the H and K lines lies within that part of the line where S_L is frequency-independent, we recognize that we cannot have a trivial rise in T_e over the region in which the central core of the H and K lines are formed. From our crude results, T_e would appear to be at least some 2×10^4 ° K.

We note that the separation of the two maxima in the emission cores are functions of T_e(max.), τ_{Cm}, ϵ and r_0, depending more strongly on the latter two. The height of the maxima also depends strongly on all four parameters. Thus it is most premature to conclude with Wilson (1957) that his observed correlation between absolute magnitude and separation of the K2 maxima reflects uniquely a correlation of turbulence with absolute magnitude. Rather, one should seek to investigate the expected dependence of this width upon the chromospheric parameters just mentioned, in addition, of course, to any turbulence effects. We defer consideration of this problem to a later paper.

b) The Hydrogen Balmer Lines

Using equations (1)–(4), we may compute the class into which the hydrogen Balmer lines fall. The chromospheric region where these Fraunhofer lines arise is likely to be locally opaque in the Lyman lines (Athay and Thomas 1958), in which case detailed balance in the Lyman-line optical transitions applies, and one readily shows that under these conditions the lowest subordinate transition (i.e., Hα for the Balmer lines) shows the same behavior as the resonance lines. The only exception is a term arising from collisional excitation from the ground state of the atom. The rate of such collisional excitations depends upon the occupation number of the ground state, which, in turn, depends upon the opacity in the Lyman continuum. Summarizing our earlier work on this problem, we estimate that, so long as the ηB^* term exceeds a few per cent of the $\int \bar{I}_\nu \varphi_\nu d\nu$ term, the effect of the collisional term from the ground state may be neglected. The energies, X_{12} and X_1, in this lowest subordinate line, Hα, are, respectively, 1.9 and 3.4 ev, which places it in the photoelectric class and not in the collisional class, as we erroneously took it to be in Paper II.

Since, as we have discussed in detail earlier (Athay and Thomas 1958), the behavior of the source functions for the whole Balmer series depends principally upon the behavior of the non-equilibrium factor b_2, we expect the S_L for the whole Balmer series to follow that of Figure 3. Because the detail of the curve depends upon r_0, we must, of course, admit the possibility of a numerical change in the $S_L(\tau_C)$-curve from one line to the next, although the form of the curve should not change.

In Figure 4 we once more reproduce our empirical results (Athay and Thomas 1958) on the source function referred to that in the H^- continuum. We show Minnaert's model photosphere out to $\tau_C = 0.1$, then a modification corresponding to $T_e(\text{min.}) = 4000°$ occurring at $\tau_C = 0.01$. In Figure 3 we used $T_e(\text{min.})$ at $\tau_C = 0.01$, but it is clear that the *type* of behavior of S_L relative to S_C will not change under a change of $\tau_C[T_e(\text{min})]$. Thus we consider that we have some understanding of the qualitative behavior of S_L for the Balmer lines. Detailed calculations are required before we try to interpret the empirical S_L in terms of the structure of the solar chromosphere. It is, however, clear that one can hardly reconcile these results with the assumption of local thermodynamic equilibrium for the formation of at least the central core of any of the early Balmer lines.

Since the free-bound absorption coefficient at the Balmer continuum limit is about 10^{-17}, it is clear from Figure 4 that the $\mathfrak{L}$ term refers to a region well below $T_e(\text{min.})$ and therefore that our approximations of constant $\mathfrak{L}$ and $\mathfrak{L}/S_1 = 0.05$ are reasonable ones for this qualitative assessment of the expected behavior of the Balmer lines.

These arguments depend upon the assumption that ηB^* exceeds the collisional term linking the first and second levels. If this assumption is not correct, the problem must be reconsidered. The collision cross-sections used in our earlier work would seem to be high, in the light of current experimental work; so we believe the conclusions we have reached on the Balmer lines to be essentially correct.

REFERENCES

Athay, R. G., and Thomas, R. N. 1958, *Ap. J.*, **127**, 96.
Jefferies, J. T., and Thomas, R. N. 1958, *Ap. J.*, **127**, 667 (Paper II).
Minnaert, M. 1953, *The Sun*, ed. G. P. Kuiper (Chicago: University of Chicago Press), p. 127.
Thomas, R. N. 1957, *Ap. J.*, **125**, 260 (Paper I).
Wilson, O. C. 1957, *Ap. J.*, **126**, 525.